

Selective targeting of perivascular macrophages for clearance of β -amyloid in cerebral amyloid angiopathy

Cheryl A. Hawkes^a and JoAnne McLaurin^{a,b,1}

^aCentre for Research in Neurodegenerative Diseases and ^bDepartment of Laboratory Medicine and Pathobiology, University of Toronto, Toronto, Ontario, Canada M5S 3H2

Edited by Don W. Cleveland, University of California at San Diego, La Jolla, CA, and approved November 26, 2008 (received for review June 6, 2008)

Cerebral amyloid angiopathy (CAA), the deposition of β -amyloid ($A\beta$) peptides in leptomeningeal and cortical blood vessels, affects the majority of patients with Alzheimer's disease (AD). Evidence suggests that vascular amyloid deposits may result from impaired clearance of neuronal $A\beta$ along perivascular spaces. We investigated the role of perivascular macrophages in regulating CAA severity in the TgCRND8 mouse model of AD. Depletion of perivascular macrophages significantly increased the number of thioflavin S-positive cortical blood vessels. ELISA confirmed that this increase was underscored by elevations in total vascular $A\beta_{42}$ levels. Conversely, stimulation of perivascular macrophage turnover reduced cerebral CAA load, an effect that was not mediated through clearance by microglia or astrocytes. These results highlight a function for the physiological role of perivascular macrophages in the regulation of CAA and suggest that selective targeting of perivascular macrophage activation might constitute a therapeutic strategy to clear vascular amyloid.

As many as 90% of all Alzheimer's disease (AD) cases present with cerebral amyloid angiopathy (CAA), the deposition of β -amyloid ($A\beta$) in cortical and leptomeningeal blood vessels (1). The vascular $A\beta$ deposits observed in AD have been shown in vitro to induce degeneration of human and murine cerebrovascular smooth muscle and endothelial cells and in vivo to inhibit angiogenesis, impair vascular tone, and decrease total cerebral blood flow (2, 3). Pathological examination of AD brains positive for CAA has revealed capillary fragmentation, thickening, and reduplication of vascular basement membranes and disruption of blood-brain barrier (BBB) permeability (4). More recently it has been demonstrated that external vessel diameter, vessel wall thickness, and luminal area were decreased by more than 50% in patients with AD with disease duration exceeding 10 years compared with individuals diagnosed 5 years before autopsy (5). Clinically, the degree of CAA severity correlates with intracerebral hemorrhage, ischemic necrosis, and degree of dementia (6).

Impaired clearance of $A\beta$ from the brain is thought to be one of the main causes of amyloid accumulation in sporadic AD. Several endogenous mechanisms exist for the removal of soluble $A\beta$ from the central nervous system (CNS) to the periphery, including receptor-mediated clearance at the BBB and via bulk movement of interstitial fluid.

In addition to putative problems with receptor-mediated $A\beta$ transport across the BBB, it has been hypothesized that CAA might arise as a result of impaired clearance of cerebral $A\beta$ along perivascular spaces (7). This suggestion is supported by histological studies of AD brains that have identified $A\beta$ deposits in dilated perivascular spaces and within small intracortical vessels and arteries, a pattern consistent with drainage pathways nearest to the brain (7). Further, dextran and ovalbumin tracers injected into the interstitial fluid of the brain parenchyma, which distribute in patterns identical to those of vascular amyloid deposited in CAA, are taken up by perivascular macrophages within 3 to 24 h after injection (8). Interestingly, reports from both human and animal anti- $A\beta$ immunization studies have demonstrated increased CAA load to be associated with cortical $A\beta$ plaque removal (9).

The perivascular spaces are an extension of the subpial space and are bordered peripherally by the basement membrane of the glia limitans and centrally by the outer surfaces of cerebral blood vessels (10). A heterogeneous population of cells reside within the perivascular spaces, including leptomeningeal mesothelial cells and macrophages, which, in combination with pericytes and astrocytic foot processes, contribute to the formation of the immune BBB (10). Perivascular macrophages are a group of innate immune cells that are distinguished from parenchymal microglia by their possession of acid phosphatase, nonspecific esterase activity, and expression of the hemoglobin-haptoglobin scavenger receptor CD163 and the mannose receptor CD206 (11, 12). Unlike parenchymal microglia, which exhibit very little turnover, perivascular macrophages are regularly replaced from the bone marrow at a rate of $\approx 30\%$ over 3 months (13). Although the full extent of the physiological role is not known, perivascular macrophages have been shown to act as antigen presenting cells, perform phagocytosis, and respond to transient CNS and peripheral inflammation (14, 15).

Recently, Fiala *et al.* (16) reported that blood-derived macrophages from patients with AD were less effective at phagocytosing $A\beta_{42}$ than those from nondemented individuals. Given that perivascular macrophages are constitutively phagocytic, and in light of their localization within perivascular spaces and proximity to vascular amyloid, we hypothesized that perivascular macrophages play a role in regulating the deposition of vascular $A\beta$. To test this hypothesis, we examined the effect of perivascular macrophage depletion and turnover on CAA severity in the TgCRND8 mouse model of AD (17). The pattern of vascular amyloid deposition in leptomeningeal and small cortical blood vessels observed in these mice mirrors that typically found in human CAA.

Results

Depletion of Perivascular Macrophages Increases CAA Severity. The use of liposome-encapsulated clodronate, an intracellular toxin, has been well characterized to study the effects of peripheral macrophage depletion and has more recently been adapted to examine the innate immune response to CNS injury (18, 19). To assess the effect of selective perivascular macrophage depletion on CAA severity, we injected clodronate- or vehicle-encapsulated liposomes into the left lateral ventricle of 4-month-old TgCRND8 mice expressing a mild degree of CAA (clodronate, $n = 32$; vehicle, $n = 30$). Clodronate administration significantly reduced the number of perivascular macrophages throughout both ipsi- and contralateral brain regions, including cortical and hippocampal areas, as dem-

Author contributions: C.A.H. and J.M. designed research; C.A.H. performed research; C.A.H. and J.M. analyzed data; and C.A.H. and J.M. wrote the paper.

The authors declare no conflict of interest.

This article is a PNAS Direct Submission.

¹To whom correspondence should be addressed. E-mail: j.mclaurin@utoronto.ca.

This article contains supporting information online at www.pnas.org/cgi/content/full/0805453106/DCSupplemental.

© 2009 by The National Academy of Sciences of the USA

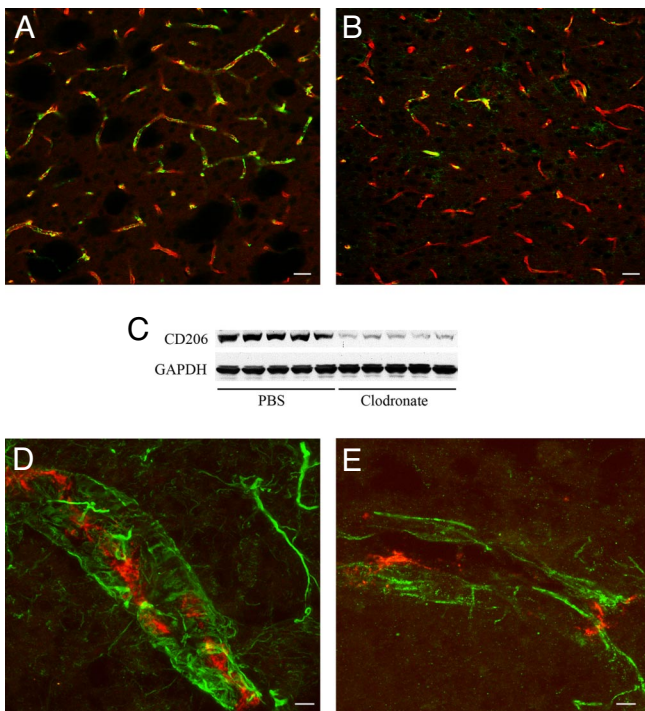


Fig. 1. Administration of liposome-encapsulated clodronate depletes perivascular macrophages. (A and B) TgCRND8 mice injected with PBS liposomes (A) showed more CD163-positive perivascular macrophages (green) associated with GLUT-1-immunoreactive (red) blood vessels in the caudate putamen than those that received clodronate-containing liposomes (B). (C) Immunoblotting of right brain homogenates (30 μ g/lane) demonstrated a significant reduction in CD206 levels ($P = 0.002$, $n = 5$) in mice receiving clodronate. (D and E) Photomicrographs showing that CD206 immunoreactivity is expressed by perivascular macrophages (red) but not by GFAP-immunoreactive astrocytes (D, green) or Iba1-positive microglia (E, green) in TgCRND8 mice. (Scale bars: A and B, 10 μ m; D and E, 20 μ m.)

onstrated by the relative absence of macrophage-specific marker CD163 immunoreactivity in clodronate-treated animals compared with controls [Fig. 1A and B and supporting information (SI) Fig. S1A and B]. This reduction was quantitatively confirmed by a $56\% \pm 4.5\%$ reduction in levels of the macrophage-specific protein CD206 between animals administered clodronate versus those receiving vehicle ($P = 0.002$; Fig. 1C).

Although macrophages are known to express the CD206 receptor, there are conflicting reports on cell-specific expression within the adult CNS (11, 20). To confirm the localization of CD206 expression to perivascular macrophages in our mouse model, we performed double labeling immunocytochemistry with anti-CD206 receptor and anti-gial fibrillary acidic protein (GFAP) or anti-ionized calcium-binding adaptor molecule-1 (Iba1) antisera to rule out astrocyte and microglia expression, respectively. Under our conditions, CD206 receptor expression was expressly localized to perivascular macrophages, whereas no co-localization was noted between CD206 receptor expression and GFAP-positive astrocytes (Fig. 1D). Iba-1-immunoreactive processes were stained around blood vessels (Fig. S1C), but did not co-localize with CD206-positive macrophages within the perivascular space (Fig. 1E and Fig. S1D).

To determine the effect of perivascular macrophage depletion on cortical CAA severity, brain sections were stained with thioflavin S (thioS) to detect A β . ThioS is one of the two accepted dyes used to visualize pathologically relevant amyloid plaques, but does not bind monomeric A β . No differences in the number or intensity of thioS-positive blood vessels were detected between untreated animals and those that received vehicle-encapsulated liposomes (Fig.

2A and B), indicating that the surgery itself did not alter amyloid deposition. Administration of clodronate liposomes and the subsequent loss of perivascular macrophages resulted in a 5-fold increase in the percentage of total cortical area covered by thioS-positive blood vessels (vehicle, $0.05\% \pm 0.005\%$; clodronate, $0.28\% \pm 0.05\%$; $P = 0.009$; Fig. 2C and D). The degree of vessel staining was also increased in clodronate-treated mice. Expression of endothelial basement membrane proteins such as perlecan and fibronectin have previously been shown to be up-regulated in association with increased CAA and may also bind to thioS (21). To determine whether basement membrane protein expression was affected by clodronate treatment and to confirm the specificity of thioS binding to amyloid deposits, we performed double labeling of thioS staining in conjunction with perlecan or fibronectin. No changes were noted in the immunoreactivity of perlecan (Fig. 2E and F) or fibronectin (data not shown) between vehicle- (Fig. 2E) and clodronate-treated (Fig. 2F) animals. Further, double labeling experiments demonstrated that, although thioS and perlecan were expressed within the same blood vessel, no co-localization was observed. These results suggest that the clodronate-induced increase in thioS-positive cortical blood vessels was caused by an up-regulation of vascular amyloid deposition.

Perivascular Macrophage Depletion Increases Vascular Levels of A β_{42} .

To confirm that vascular amyloid was specifically increased, we performed double labeling immunocytochemistry of brain tissues with anti-A β_{8-17} (clone 6F/3D) and anti- α -smooth muscle actin. Similar to the thioS staining, clodronate-treated mice showed a greater number of A β -positive blood vessels throughout the cortex compared with vehicle-injected animals (Fig. S2A–D). We next examined whether A β_{40} or A β_{42} was preferentially deposited following clodronate treatment. No appreciable differences in the amount or intensity of vascular A β_{40} immunoreactivity were noted between vehicle- (Fig. 2G) and clodronate-treated tissue sections (Fig. 2H). These histological results were confirmed by sandwich ELISA, in which no differences were detected in total A β_{40} levels in isolated blood vessels (vehicle, 23.8 ± 1.6 ng/g; clodronate, 21.5 ± 2.4 ng/g; $P = 0.21$), vessel-depleted cortex (vehicle, 18.4 ± 1.0 ng/g; clodronate 17.6 ± 1.5 ng/g; $P = 0.32$) or plasma (vehicle, $3,462 \pm 84.8$ pg/mL; clodronate, $3,569 \pm 185.8$ pg/mL; $P = 0.29$) from the two treatment groups. By contrast, brain sections from clodronate-treated TgCRND8 mice exhibited an increase in the number of cortical vessels positive for anti-A β_{42} immunoreactivity compared with vehicle-injected animals (Fig. 2I and J). An increase in the intensity of anti-A β_{42} staining was also noted in clodronate-treated animals. Similarly, ELISA results showed a significant increase in total A β_{42} levels in blood vessels isolated from clodronate-treated mice versus controls ($P = 0.03$; Fig. 2K). Interestingly, A β_{42} levels were decreased in the corresponding cortical samples ($P = 0.04$; Fig. 2L), whereas plasma concentrations were not different between the two treatment groups ($P = 0.29$; Fig. 2M). Quantification of A β_{8-17} -positive plaques confirmed the significant decrease in cortical plaque load in clodronate-treated mice versus controls (vehicle, $0.004\% \pm 0.001\%$ of cortex covered; clodronate, $0.002\% \pm 0.0003\%$; $P = 0.04$). These data would thereby suggest that perivascular macrophage depletion in TgCRND8 mice induces a preferential vascular deposition of A β_{42} peptides, whereas A β_{40} levels are relatively unaffected. Although human CAA consists predominantly of A β_{40} , these results are not surprising given the preferential expression and amyloidogenic properties of A β_{42} in the TgCRND8 mouse.

To determine whether macrophage depletion had an effect on microglial activation, Iba-1 expression was assessed in clodronate-injected TgCRND8 mice. Iba-1-positive activated microglia were identified throughout the parenchyma and surrounding the vasculature in the brains of vehicle- and clodronate-injected mice (Fig. 2N and O). However, no quantitative difference in Iba-1 levels was found between mice treated with vehicle- or clodronate-containing

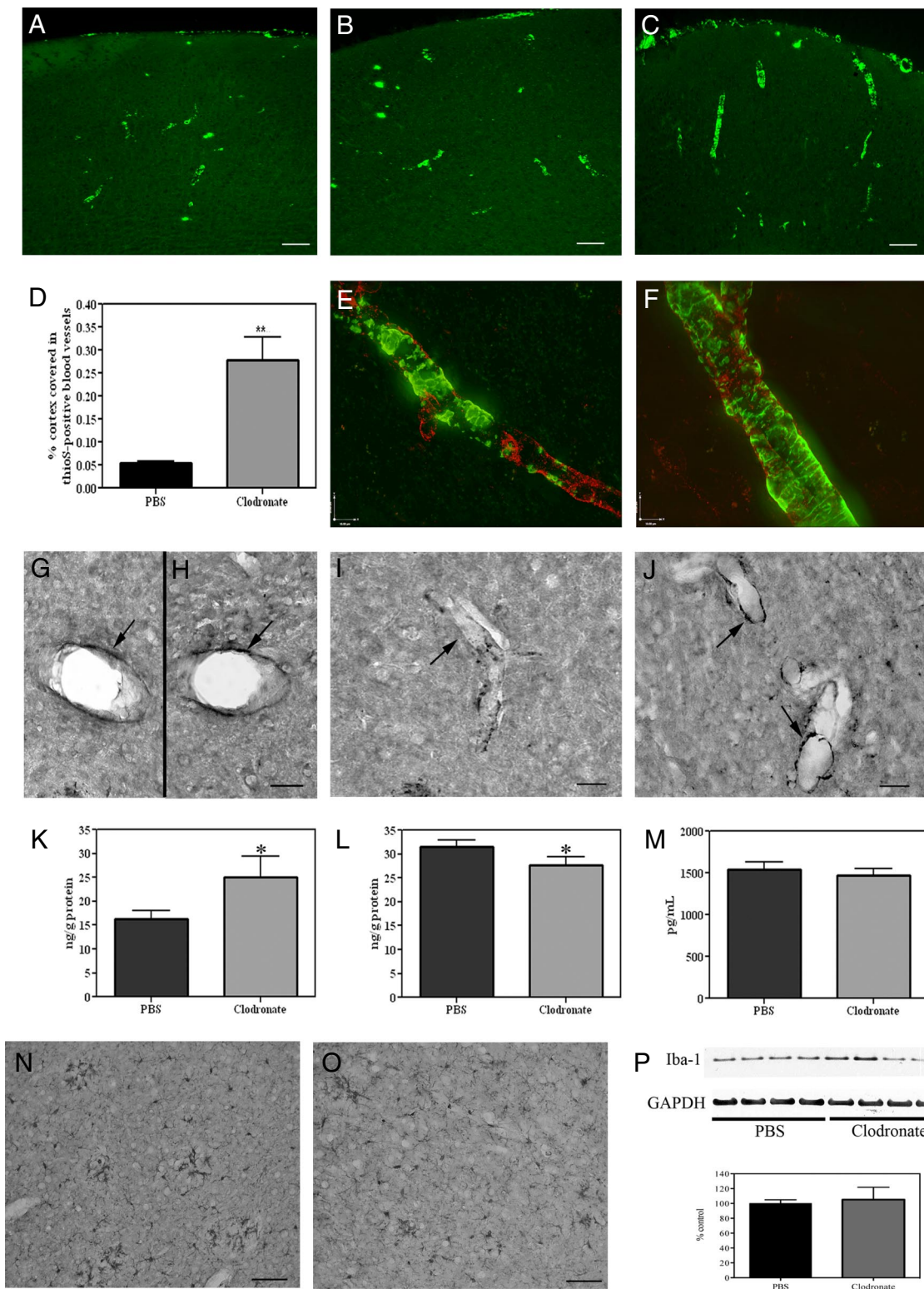


Fig. 2. Depletion of perivascular macrophages increases CAA severity. (A–C) Naive TgCRND8 mice (A) and those treated with PBS solution (B) show fewer thioS-positive cortical blood vessels than clodronate-treated mice (C). (D) Total cortical area covered in thioS-positive blood vessels was increased 5-fold in clodronate-treated animals ($P = 0.01$, $n = 10$). (E and F) No colocalization was found between thioS (green) and anti-perlecan (red) staining in PBS solution- (E) or clodronate-treated mice (F). (G and H) No differences in $A\beta_{40}$ -positive staining were noted between vehicle- (G) and clodronate-treated animals (H). (I and J) The number and intensity of $A\beta_{42}$ -positive cortical blood vessels was increased in mice treated with clodronate (J) versus control animals (I). (K–M) Total human $A\beta_{42}$ levels in cortical blood vessels isolated from clodronate-treated mice (K) were significantly increased ($P = 0.03$, $n = 12$) compared with PBS solution-injected animals. $A\beta_{42}$ levels were significantly decreased in the cortical samples (L; $P = 0.04$, $n = 12$) of clodronate-treated animals, but were not altered in plasma samples (M; $P = 0.29$). (N–P) Iba-1-positive microglia were noted throughout the cortex of vehicle- (N) and clodronate-treated mice (O). No differences were noted in Iba-1 levels (P) between treatment groups ($P = 0.54$, $n = 4$). Values represent mean \pm SEM of samples analyzed in triplicate; * $P < 0.05$ and ** $P < 0.01$. (Scale bars: A–C, 75 μ m; E and F, 10 μ m; G–J, 20 μ m; N and M, 70 μ m.)

liposomes (Fig. 2*P*; $P = 0.54$). These data indicate that perivascular macrophage depletion did not significantly alter microglial activity.

Increases in CAA severity have been associated with increases in micro-hemorrhages in human studies and animal models of AD (9, 22). To investigate the impact of increased $A\beta_{42}$ deposition on cerebral “microbleeds,” we examined brain tissues for the hemoglobin breakdown product hemosiderin by Prussian blue staining (9). Despite the significant increase in vascular amyloid following clodronate treatment, we were unable to detect Prussian blue labeling of blood vessels in vehicle- or clodronate-treated animals. Staining was evident only along the tract mark at the site of injection and could be distinctly identified within microglial cells (Fig. S2 *E* and *F*). As such, no differences in Prussian blue staining were noted between clodronate- and vehicle-injected animals, suggesting that increased CAA did not compromise vascular integrity.

Chitin Administration Stimulates Turnover of Perivascular Macrophages. Given our findings that perivascular macrophage depletion increased CAA severity, we examined the effects of perivascular macrophage turnover on vascular amyloid load. At 5 months of age, TgCRND8 mice deposit significant CAA and thus allowed for detection of treatment-induced changes. To stimulate perivascular macrophage turnover, we used chitin, a naturally occurring biopolymer of N-acetyl- β -D-glucosamine expressed in the cell walls of fungi, crustaceans, insects, and worms (chitin, $n = 21$; vehicle, $n = 20$). Chitin uptake in peripheral macrophages is believed to occur via binding to the CD206 receptor (23).

It has previously been shown that perivascular macrophages phagocytose fluorescently conjugated dextran dyes injected into the lateral ventricles of the mouse brain (15). This method can thus be used to visualize macrophage turnover following the sequential administration of red and green dyes, by determining the ratio of singly and doubly labeled cells. Although chitin is known to stimulate peripheral macrophages, its effect on perivascular macrophages has not been determined. To examine the effect of chitin administration on perivascular macrophage turnover in the presence of significant CAA load, we injected $5 \mu\text{g}$ of chitin or PBS solution plus dextran-conjugated fluorescein into the left lateral ventricle of 5-month-old TgCRND8 mice, followed 2 weeks later by a second injection of chitin or PBS plus dextran-conjugated Alexa Fluor 594. Dextran dyes were selectively taken up by macrophages that localized only to the perivascular space (Fig. 3*A* and *B* and Fig. S3*A*). The majority of perivascular macrophages in vehicle-injected mice exhibited both red and green dextran dyes, indicating little macrophage turnover during the experimental period (Fig. 3*A*). Conversely, significantly more singly labeled red macrophages were noted in chitin-treated mice (Fig. 3*B*; vehicle, $32.7\% \pm 2.4\%$ red cells; chitin, $48.3\% \pm 5.9\%$; $P = 0.01$), suggesting that turnover of perivascular macrophages was stimulated by chitin administration and that CAA deposition did not inhibit this effect. No difference was noted in CD206 levels between chitin- and vehicle-injected animals, indicating a constant rate of perivascular macrophage turnover ($P = 0.31$; Fig. S3*B*).

Stimulation of Perivascular Macrophage Turnover Promotes Clearance of CAA. To induce a sustained increase in macrophage turnover, animals were injected with chitin twice over the 30-day experimental period, following which thioS staining was performed to examine CAA severity. Consistent with results from the clodronate study, thioS labeled vascular amyloid throughout the cortex and leptomeninges of TgCRND8 mice injected with vehicle (Fig. 3*C*). Treatment with chitin caused a significant reduction in the intensity of staining and the number of thioS-labeled cortical blood vessels compared with vehicle-injected mice (vehicle, $0.29\% \pm 0.06\%$ cortical area covered; chitin, $0.10\% \pm 0.02\%$; $P = 0.007$; Fig. 3*D* and *E*). To verify that the clearance of vascular amyloid was mediated by perivascular macrophages, we examined brain sections from chitin-treated animals for colo-

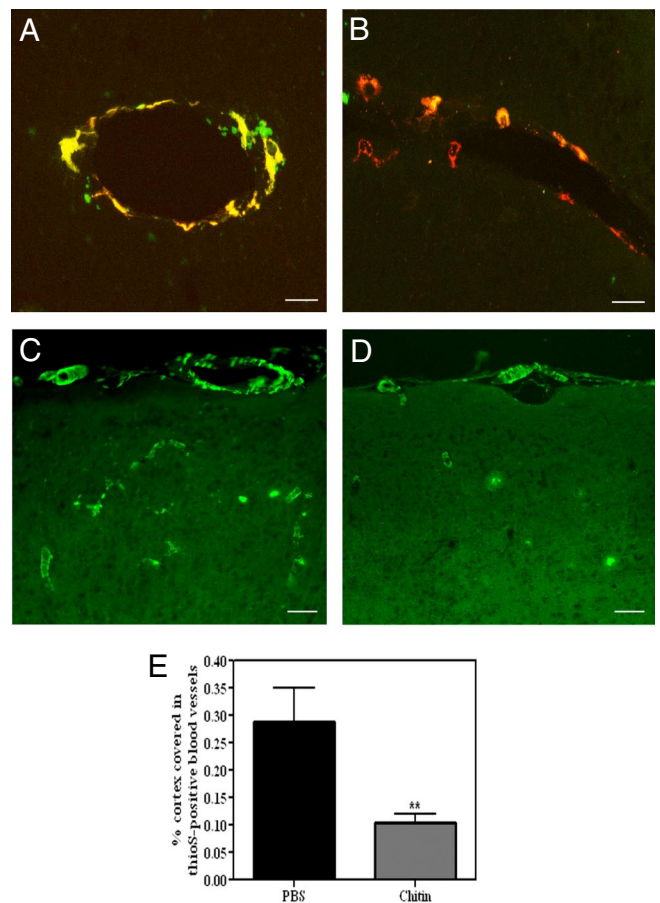


Fig. 3. Chitin administration stimulates perivascular macrophage turnover and clears CAA. (*A* and *B*) Most cells in PBS-treated mice showed colocalization of red and green dextran dyes (*A*, yellow-labeled cells), whereas chitin-treated animals (*B*) showed numerous singly, red-labeled macrophages ($P = 0.01$, $n = 4$). (*C*–*E*) The number of thioS-positive cortical blood vessels was significantly decreased following chitin treatment (*D*) compared with PBS solution-injected mice (*C*) (*E*, $P = 0.01$, $n = 10$). Histograms represent mean \pm SEM values obtained from 3 brain sections per animal; $**P < 0.01$. (Scale bars: *A* and *B*, $10 \mu\text{m}$; *C* and *D*, $75 \mu\text{m}$.)

calization of $A\beta$ with perivascular macrophages, reactive astrocytes, or activated microglia. No colocalization was observed between GFAP-positive astrocytes or their end feet projections (Fig. 4*A*). Similarly, although activated, Iba1-immunoreactive microglia were clearly found to be associated with parenchymal plaques (Fig. 4*B*, arrows), no such association was observed between microglia and vascular amyloid. By contrast, CD163-positive macrophages demonstrated positive co-localization with thioS-stained amyloid in cortical and leptomeningeal vessels (Fig. 4*C*). These results suggest that chitin-induced reduction of CAA load was mediated via uptake by perivascular macrophages, rather than by activated microglia or reactive astrocytes.

To confirm that increased perivascular macrophage turnover specifically cleared vascular amyloid, brain sections were stained for anti- $A\beta_{8-17}$ and anti- α -smooth muscle actin. Chitin-treated mice showed a decrease in the number of $A\beta$ -positive blood vessels throughout the cortex compared with vehicle-injected animals (Fig. S3 *C* and *D*). Given the preferential effect of perivascular macrophage depletion on $A\beta_{42}$, we next investigated whether an $A\beta_{42}$ effect was also observed following perivascular macrophage turnover. Consistent with results from the clodronate experiments, no differences in $A\beta_{40}$ -immunoreactivity were observed between chitin- (Fig. 4*E*) and vehicle-treated mice (Fig. 4*D*). These findings are in contrast to anti- $A\beta_{42}$ staining, which revealed a notable

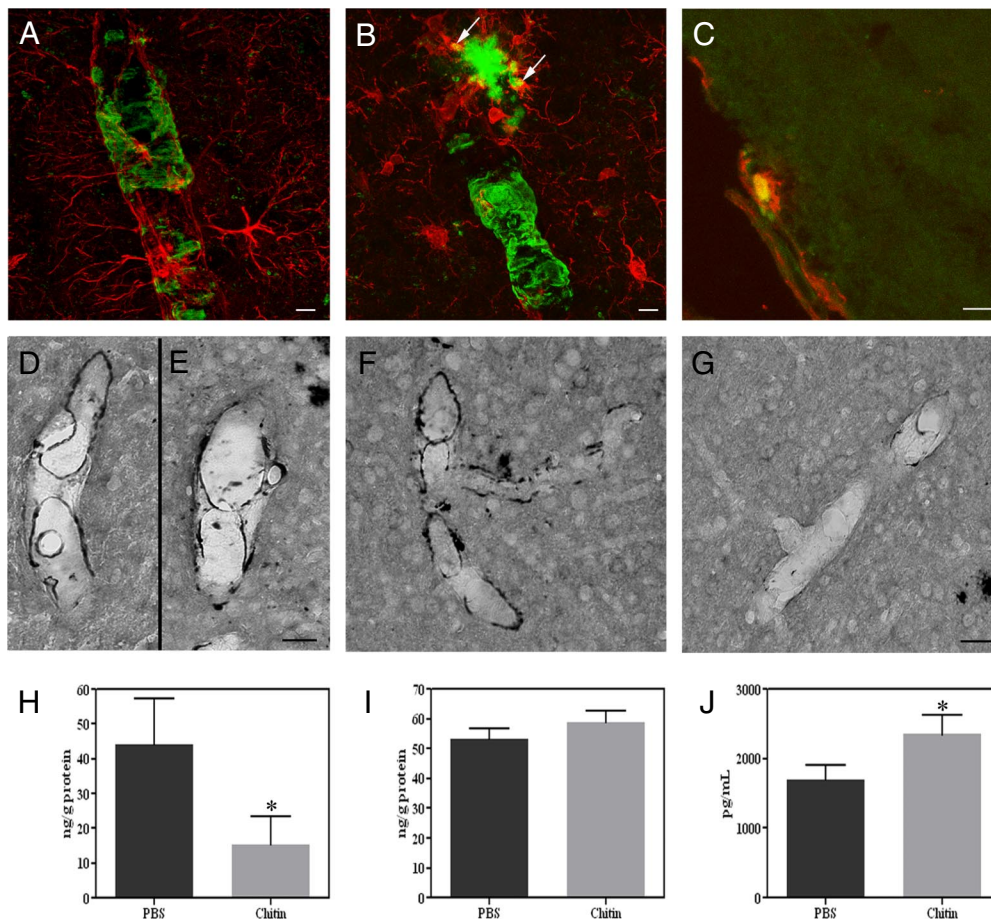


Fig. 4. Perivascular macrophages clear CAA. (A–C) Chitin-treated mice showed no colocalization between thioS (A–C, green) and GFAP-positive astrocytes (A, red), nor with Iba1-positive microglia (B, red), which were however associated with parenchymal amyloid plaques (B, arrows). However, CD163-immunoreactive macrophages (C, red) colocalized with thioS-labeled vascular amyloid (C, green) in these mice. (D–G) No differences were noted between vehicle- (D) and chitin-treated animals (E) in brain tissue sections processed for anti- $A\beta_{40}$ staining. A significant reduction in $A\beta_{42}$ -positive staining (F and G) was noted in chitin-treated animals (G) compared with controls (F). (H–J) Total human $A\beta_{42}$ levels were significantly decreased in blood vessels (H, $P = 0.04$) and plasma samples (J, $P = 0.04$, $n = 6$) isolated from chitin-treated mice, but not in vessel-depleted cortical samples (I, $P = 0.16$). Values represent mean \pm SEM of samples analyzed in triplicate; * $P < 0.05$. (Scale bars: A and B, 5 μ m; C, 25 μ m; D–G, 20 μ m.)

decrease in the degree of vessel staining, as well as the total number of $A\beta_{42}$ -labeled blood vessels in mice treated with chitin versus vehicle (Fig. 4 F and G). Further, CD163-positive perivascular macrophages colocalized with anti- $A\beta_{42}$ -positive amyloid in cortical and leptomeningeal vessels of chitin-treated mice (Fig. S3E). These histological findings were confirmed by a significant reduction in total $A\beta_{42}$ levels in blood vessels isolated from the cortices of chitin-treated animals ($P = 0.04$; Fig. 4H). No changes in $A\beta_{42}$ levels were detected in vessel-depleted cortical samples between treatment groups ($P = 0.16$; Fig. 4I), which was confirmed by histological quantification of cortical $A\beta$ plaque load (vehicle, $0.24\% \pm 0.03\%$ of cortex covered; chitin, $0.27\% \pm 0.04\%$; $P = 0.61$). Plasma $A\beta_{42}$ levels were significantly increased in mice injected with chitin ($P = 0.04$; Fig. 4J). As expected, no differences in total $A\beta_{40}$ levels were observed between chitin- and vehicle-treated groups in blood vessels (vehicle, 37.6 ± 9.1 ng/g; chitin, 40.2 ± 8.1 ng/g; $P = 0.42$), cortex (vehicle, 37.5 ± 6.6 ng/g; chitin, 35.8 ± 4.1 ng/g; $P = 0.42$), or plasma (vehicle, $4,736 \pm 343.5$ pg/mL; chitin, $4,970 \pm 492.9$ pg/mL; $P = 0.36$). To confirm that chitin treatment did not stimulate microglial activation, Iba-1 expression was assessed. Immunocytochemical examination revealed no differences in the number of Iba-1-positive activated microglia throughout the parenchyma and microvasculature between treatment groups (Fig. S4A and B). Further, no quantitative differences

in Iba-1 levels were found between mice treated with vehicle or chitin ($P = 0.91$; Fig. S4C). These results are consistent with a role of perivascular macrophage-mediated clearance of $A\beta$ from the cerebral vasculature.

Discussion

The role of vascular dysregulation in the etiology of AD dementia is increasingly becoming a topic of research. $A\beta$ peptides have been shown to cause vasoconstriction and intraluminal thickening and induce smooth muscle cell death, thereby increasing the risk of cerebral hemorrhage and stroke (2, 4, 5). However, the pathogenesis of CAA has not been fully addressed experimentally. We sought to examine the role of perivascular macrophages in the clearance of CAA from cortical blood vessels of the TgCRND8 mouse model of AD. We report that CAA severity is exacerbated following selective perivascular macrophage depletion and that the more toxic $A\beta_{42}$ peptide is predominantly altered by this treatment. Further, stimulation of perivascular macrophage turnover results in the clearance of $A\beta_{42}$ -immunoreactive and thioS-positive vascular amyloid deposits via CD163-positive macrophages. These data provide additional evidence to support a perivascular pathway for amyloid clearance and suggests that, under normal conditions, macrophages within the perivascular spaces may function to eliminate $A\beta$ peptides from the cerebral vasculature.

Our data suggests that uptake and removal of vascular amyloid by perivascular macrophages is ongoing under physiologic conditions in TgCRND8 mice and that disruption of this process exacerbates CAA severity. This is supported by the findings that (i) dextran dye-positive cells were identified in only cells with a macrophage morphology within the perivascular space and not in the parenchyma, indicating that macrophages did not migrate into the neuropil; (ii) CAA levels were reduced/exacerbated throughout all cortical areas, both ipsilateral and contralateral to the site of injection, suggesting that CAA severity was not mediated by activation or inhibition of local resident microglia; (iii) chitin administration had no effect on parenchymal plaque load or total A β levels in vessel-depleted cortical samples; and (iv) thioS- and A β ₄₂-positive vascular amyloid co-localized with CD163-positive macrophages, but not with Iba1-positive microglia or GFAP-positive astrocytes. However, given the complex interplay among all immune cells, a possible cooperative action between perivascular macrophages and microglia or astrocytes in the regulation of CAA cannot be completely discounted.

At present, there are no therapeutic strategies for the management of CAA. However, the importance of CAA and its interrelationship with parenchymal amyloid was underscored recently by reports from animal and human anti-A β immunization studies, in which reductions in parenchymal plaque load were associated with significant increases in CAA severity and brain micro-hemorrhages in amyloid-laden vessels (9). We did not find an increase in cerebral bleeding incidence associated with clodronate treatment in the present experiment, as a result of the age of our animals and the relatively short duration of treatment; however, CAA-associated micro-hemorrhages remain a major therapeutic concern. Although much more work is needed to characterize the inflammatory response of perivascular macrophage stimulation in the AD brain, in the present study, chitin administration was well tolerated by TgCRND8 mice expressing moderate CAA pathology and no deleterious side effects were noted following stimulation of perivascular macrophage turnover. Thus, the current findings suggest that perivascular macrophages might be a potential target for therapeutic intervention in the clearance of CAA.

Methods

Animals. TgCRND8 mice overexpressing the human Swedish (KM670/671NL) and Indianan (V717F) APP mutations under a hamster prion protein promoter were maintained on an outbred C3H/57BL6 background (17). Mice were age- and sex-matched and allowed food and water ad libitum. All experiments were performed in accordance with the guidelines stipulated by the University of Toronto and Canadian Council for Animal Care.

- Attems J, Lauda F, Jellinger KA (2008) Unexpectedly low prevalence of intracerebral hemorrhages in sporadic cerebral amyloid angiopathy: an autopsy study. *J Neurol* 255:70–76.
- Miao J, et al. (2005) Cerebral microvascular amyloid beta protein deposition induces vascular degeneration and neuroinflammation in transgenic mice expressing human vasculotropic mutant amyloid beta precursor protein. *Am J Pathol* 167:505–515.
- Shin HK, et al. (2007) Age-dependent cerebrovascular dysfunction in a transgenic mouse model of cerebral amyloid angiopathy. *Brain* 130:2310–2319.
- Perlmutter LS (1994) Microvascular pathology and vascular basement membrane components in Alzheimer's disease. *Mol Neurobiol* 9:33–40.
- Tian J, et al. (2006) Relationships in Alzheimer's disease between the extent of Abeta deposition in cerebral blood vessel walls, as cerebral amyloid angiopathy, and the amount of cerebrovascular smooth muscle cells and collagen. *Neuropathol Appl Neurobiol* 32:332–340.
- Attems J, Quass M, Jellinger KA, Lintner F (2007) Topographical distribution of cerebral amyloid angiopathy and its effect on cognitive decline are influenced by Alzheimer disease pathology. *J Neurol Sci* 257:49–55.
- Nicoll JA, et al. (2004) Cerebral amyloid angiopathy plays a direct role in the pathogenesis of Alzheimer's disease. Pro-CAA position statement. *Neurobiol Aging* 25:589–597.
- Carare RO, et al. (2008) Solutes, but not cells, drain from the brain parenchyma along basement membranes of capillaries and arteries: Significance for cerebral amyloid angiopathy and neuroimmunology. *Neuropathol Appl Neurobiol* 34:131–144.
- Pfeifer M, et al. (2002) Cerebral hemorrhage after passive anti-A β immunotherapy. *Science* 298:1379.
- Bechmann I, Galea I, Perry VH (2007) What is the blood-brain barrier (not)? *Trends Immunol* 28:5–11.
- Galea I, et al. (2005) Mannose receptor expression specifically reveals perivascular macrophages in normal, injured, and diseased mouse brain. *Glia* 49:375–384.
- Kim WK, et al. (2006) CD163 identifies perivascular macrophages in normal and viral encephalitic brains and potential precursors to perivascular macrophages in blood. *Am J Pathol* 168:822–834.
- Bechmann I, et al. (2001) Turnover of rat brain perivascular cells. *Exp Neurol* 168:242–249.
- Williams K, Alvarez X, Lackner AA (2001) Central nervous system perivascular cells are immunoregulatory cells that connect the CNS with the peripheral immune system. *Glia* 36:156–164.
- Bechmann I, et al. (2001) Immune surveillance of mouse brain perivascular spaces by blood-borne macrophages. *Eur J Neurosci* 14:1651–1658.
- Fiala M, et al. (2005) Ineffective phagocytosis of amyloid-beta by macrophages of Alzheimer's disease patients. *J Alzheimers Dis* 7:221–232.
- Chishti MA, et al. (2001) Early-onset amyloid deposition and cognitive deficits in transgenic mice expressing a double mutant form of amyloid precursor protein 695. *J Biol Chem* 276:21562–21570.
- Van Rooijen N, Sanders A (1994) Liposome mediated depletion of macrophages: Mechanism of action, preparation of liposomes and applications. *J Immunol Methods* 174:83–93.
- Polfliet MM, et al. (2001) A method for the selective depletion of perivascular and meningeal macrophages in the central nervous system. *J Neuroimmunol* 116:188–195.
- Burudi EM, Regnier-Vigouroux A (2001) Regional and cellular expression of the mannose receptor in the post-natal developing mouse brain. *Cell Tissue Res* 303:307–317.
- Wyss-Coray T, et al. (2000) Chronic overproduction of transforming growth factor-beta1 by astrocytes promotes Alzheimer's disease-like microvascular degeneration in transgenic mice. *Am J Pathol* 156:139–150.
- Patton RL, et al. (2006) Amyloid-beta peptide remnants in AN-1792-immunized Alzheimer's disease patients: A biochemical analysis. *Am J Pathol* 169:1048–1063.

Depletion of Perivascular Macrophages. Perivascular macrophage depletion was carried out according to the protocol adapted by Polfliet *et al.* (19) (see *SI Methods*). Four-month-old TgCRND8 mice were anesthetized with isoflurane and stereotactically injected with 10 μ L of PBS solution- or clodronate-containing liposomes into the left lateral ventricle (coordinates from Bregma: anteroposterior, –0.2 mm; mediolateral, 1.2 mm; dorsoventral, 2.3 mm; $n = 30$ per group). Animals were killed 1 month later and brains were processed for further analysis.

Stimulation of Perivascular Macrophage Turnover. Five-month-old TgCRND8 mice received a 5- μ L injection of either PBS solution or chitin (1 mg/mL) into the left lateral ventricle, which was repeated 14 days later ($n = 20$ per group). A subset of animals received a combination of chitin or PBS solution plus 5 μ L dextran fluorescein dye, followed 2 weeks later by an injection of chitin or PBS solution plus 5 μ L dextran Alexa Fluor 594 dye ($n = 4$ per group). Animals were killed 14 days after the last injection and brains were processed for further analysis.

Immunocytochemistry. Mice were deeply anesthetized with sodium pentobarbital and perfused with 0.1 M PBS solution (pH 7.4) and 10% formalin or snap-frozen. Sections (20 μ m) were incubated overnight with anti-CD163 (1:500), anti-Iba-1 (1:1,000), anti-A β _{8–17} (1:500), or anti-A β _{40/42} (1:70) and developed by using the glucose oxidase-DAB-nickel enhancement method (see *SI Methods* for antibody sources). For thioS staining, sections were treated with 1% thioS for 5 min, differentiated twice in 70% EtOH, and washed in PBS solution. For thioS plus GFAP/Iba1/CD163/perlecan double labeling, sections were incubated overnight with anti-GFAP (1:250), anti-Iba1 (1:250), anti-CD163 (1:100), or anti-perlecan (1:100); exposed to Alex Fluor 594-conjugated anti-rabbit/mouse (1:200); and then processed for thioS staining (see *SI Methods* for additional staining procedures). Photomicrographs of visualized sections were captured by using a Zeiss AxioScope 2 Plus microscope and exported to Adobe Photoshop CS.

Immunoblotting. Right brain hemisphere homogenates were separated by 4%–20% polyacrylamide gel electrophoresis (30 μ g/lane), transferred to nitrocellulose membrane, and incubated overnight at 4°C with anti-CD163 (1:1,000), anti-CD206 (1:1,000), or anti-Iba1 (1:750) antibodies. Membranes were stripped, and re-probed with anti-GAPDH (1:10,000) to ensure equal protein loading.

Cortical Blood Vessel Isolation and A β ELISA Sample Preparation. Isolation of cortical blood vessels was adapted from Patton *et al.* (22) (see *SI Methods*). Total A β was extracted from cortical filtrates by sonicating homogenates in 70% formic acid, followed by centrifugation (100,000 $\times g$, 1 h, 4°C) and neutralization of the samples. Isolated blood vessels were washed, centrifuged (6,000 $\times g$, 10 min, 4°C) to remove supernatant, and treated similarly as cortical samples to extract total A β _{40/42}. Neutralized samples were diluted and analyzed by using commercially available sandwich ELISA kits, as per the manufacturer's instructions (BioSource, Burlington, ON, Canada). Plasma samples were also assessed for A β _{40/42} levels. Samples were measured in triplicate, with mean values \pm SEM, reported for treatment groups.

ACKNOWLEDGMENTS. The authors thank Mary Brown, Kevin DaSilva, Daniela Fenili, and Dr. Teresa DeLuca for their technical assistance. This work was supported by grants from the Canadian Institutes for Health Research (C.H., J.M.), the Natural Sciences and Engineering Research Council (J.M.), the Alzheimer's Society of Canada (C.H.), and the Ontario Alzheimer's Society (J.M.).